

Shock-induced radiation spectra of fused quartz

Ken-ichi Kondo^{a)} and Thomas J. Ahrens

Seismological Laboratory, California Institute of Technology, Pasadena, California 91125

Akira Sawaoka

Research Laboratory of Engineering Materials, Tokyo Institute of Technology, Nagatsuta, Midori, Yokohama 227, Japan

(Received 23 September 1982; accepted for publication 13 April 1983)

An optical multichannel analyzer is applied to observe shock-induced radiation spectra of fused quartz in the 23–31 GPa shock-pressure range. Characteristics of sample-driver interface strongly influence both intensity and profile of the observed spectra. Brightness and color temperature are determined by an integration of spectral radiance and a fit to the greybody radiation spectrum, respectively. The resultant brightness and color temperature are lower and considerably higher than those estimated by the theoretical calculation, respectively. Some broad but strong line spectra are, however, superimposed onto the continuous greybody radiation spectrum even though the influences of the interface are reduced as much as possible. The line spectra are probably caused by electroluminescence and/or triboluminescence.

PACS numbers: 62.50. + p, 63.90. + t, 78.60. – b

INTRODUCTION

The measurement of temperatures in shock-compressed materials is important because it provides constraints on and tests for the assumptions in the analysis of Hugoniot data in order to complete equations of state and to confirm phase transitions. A quantitative measurement of the thermal radiation from transparent media in the shock state can be used to determine shock temperature. Kormer *et al.*¹ reported such a measurement based on the brightness temperature using a two-channel time-resolved pyrometer. Recently, Lyzenga and Ahrens² developed a six-channel time-resolved pyrometer to determine the color temperature and emissivity by fitting the data to the Planck radiation function. Sugiura *et al.*³ developed a system for measuring the shock-induced radiation spectrum with 500 channels, which was integrated over a certain time interval less than shock propagation time through the sample. Kondo and Ahrens improved a similar system by calibrating the radiance sensitivity on an absolute basis.⁴ Since the dynamic range of the improved system is extended to about 20 times, a shape of the spectrum can be more precisely analyzed.

Although several researchers have measured the shock compression and shock temperature of fused quartz,^{2–9} much of the shock temperature data have been inconsistent. Therefore, we have employed the new system to observe the shock-induced radiation spectrum. In this paper, we report the observed spectrum of fused quartz in the 20–30 GPa pressure range and discuss some technical and phenomenological problems in shock temperature measurements.

EXPERIMENT

The experimental apparatus used consists of an optical multichannel analyzer (OMA2, EG and G Princeton Applied Research), a spectrometer (Jarell-Ash, 82-410), and a time-resolved pyrometer using a high-speed *PIN* photo-

diode.³ Light from the shock-compressed state passes through the uncompressed material via the shock front and is collected and focused onto the entrance slit of the spectrometer. A slit of 0.3 mm width was used in this study. The dispersed spectrum is recorded on the silicon diode target which is gated for 300 ns at appropriate times. The sample free surface is masked, leaving a 10-mm-diam window uncovered to avoid edge effects. In order to observe the time dependence of shock radiation with an oscilloscope, a small front surface mirror is placed at the side of the slit of the spectrometer so that a portion of the light would reflect into the *PIN* photodiode. Time resolution of the photodiode circuit is estimated to be 5 ns. Since the output voltage of the *PIN* photodiode circuit is not calibrated, only relative changes of light intensity as a function of time is available. Details of the apparatus are described elsewhere.⁴

The fused quartz samples studied are of stock commercial grade (Toshiba Ceramics Co., Ltd, T-1000), whose initial density is 2.201 ± 0.001 mg/m³. The disc-shaped samples are 20 mm in diameter and approximately 3 mm in thickness, and their flat surfaces were polished to optical grade. Both surfaces of a Cu-driver plate were also polished using 0.3- μ m corundum powder. The degree of flatness of the surfaces was determined using an optical flat.

The radiation resulting from the following types of sample-driver interface was investigated: (1) clear lapped and polished surfaces; (2) employing an epoxy resin less than 0.002 mm thick at the interface; (3) metal evaporation on the sample surface and using epoxy layer less than 0.002 mm thick as well as in (2). Two self-shortening pins were mounted on the driver plate to provide a trigger pulse by which the entire system was triggered.

Shock experiments were conducted using a 40-mm bore propellant gun of Caltech. The sample assembly was impacted by a tungsten flyer plate embedded in a Lexan plastic sabot. The velocity of the projectile was measured by laser interruption and flash x-ray shadowgraph techniques. The thermodynamical parameters of the generated shock state

^{a)} Present address: RLEM, Tokyo Institute of Technology.

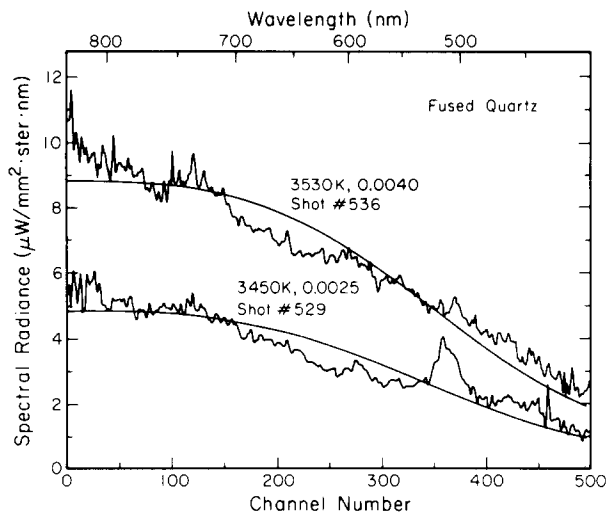


FIG. 1. Spectral radiances of shock compressed fused quartz at 23.0 and 29.8 GPa for shot Nos. 529 and 536, respectively. The smooth curves were obtained by least squares fit to the greybody radiance equation on which the color temperature and emissivity are indicated.

were determined by the impedance match method using the Hugoniot data of fused quartz,^{8,10} copper and tungsten.¹¹ A theoretical continuum temperature, calculated based on the adiabatic thermodynamic path and the Hugoniot in the mixed phase region, closely corresponded with temperatures calculated previously.¹²

RESULTS AND DISCUSSIONS

The characteristics of the interface between the sample and the Cu-driver plate strongly influenced the observed spectrum and time-dependent profile as described later. The most consistent spectra were obtained in the case of (3), where the sample surface was plated via evaporation to form an opaque layer of silver. The epoxy resin was also applied between the sample and the Cu-driver plate. The typical observed spectra at 23.0 and 29.8 GPa (Fig. 1) are fit with greybody radiation Plank's equations of the form:

$$B(\lambda) = C_1 \lambda^{-5} [\exp(C_2/\lambda T) - 1]^{-1},$$

where $C_1 = 1.191 \times 10^{-16}$ (W m²/sr), $C_2 = 1.439 \times 10^{-2}$ (m K), and λ is the wavelength in vacuum. The resultant color temperatures for both experiments are very high with a small value of emissivity, as shown in Fig. 1. The brightness temperatures are also estimated, integrating the

intensity from 452 to 751 nm wavelength and comparing it with the integrated value of the Plank's radiation equation. Experimental conditions and results are summarized in Table I. The higher temperature limit of the sixth column in Table I implies the hypothetical temperature which is calculated by ignoring the phase transition energy to stishovite because of its ambiguity. The expected temperature is higher than the brightness one but quite lower than the color one. The brightness temperatures obtained here are in good agreement with the extrapolated values from those of Sugiura *et al.*⁹ The high color temperature with low emissivity obtained here strongly suggests the heterogeneous radiation which is produced by localized deformation in brittle materials. The heterogeneous radiation mechanism can be explained by a shear instability model.⁴

However, it is clearly seen for shot No. 529 in Fig. 1 that some broad but strong line spectra are superimposed onto the continuous radiation spectrum, and that the color temperature is strongly influenced by such spectra. The wavelengths of the strongest and the second emission bands are 509 and 589 nm, respectively. The influence decreases at high pressure (see shot No. 536). The broad peak in the vicinity of 730 to 740 nm wavelength range seems to be an artifact of our radiance sensitivity calibration because it appears in every experiments.⁴ In the calibration, to reduce the radiance of a standard tungsten lamp down to the levels of these experiments, we used a neutral density filter (Kodak 96). Unfortunately the transmittance of this filter has a feature in the 730–740 nm range.

Recent measurements of electrical resistivity and shock-induced polarization of fused quartz indicate a marked decrease of resistivity ~ 10 – 0.1Ω m at a shock pressure ~ 40 GPa.¹² Up to the transition pressure, electrical resistivity linearly decreases with inverse temperature at an activation energy of 0.88 eV, which corresponds to that of fused quartz at ambient conditions. After the transition, electrical resistivity also linearly decreases with inverse temperature at an activation energy of 2.4 ± 0.5 eV.¹² The above emission bands correspond to 2.44 and 2.10 eV, respectively, and are close to such activation energy. If we assume that the electron level of 2.4 ± 0.5 eV in the gap is produced during shock compression, it should be an acceptor bound level or an electron trap because the polarization signals suggest a positive carrier. It is also likely that the activated free-atomic state exists between quartz and stishovite (four- and six-fold coordinated SiO₂) in the mixed phase region, when a change

TABLE I. Summary of shock-induced radiation measurements of fused quartz.

Shot number	Sample thickness [mm]	Projectile velocity [mm/μs]	Shock pressure [GPa]	Expected temperature [K]	Higher limit [K]	Color temperature [K]	Emissivity [–]	Brightness temperature [K]	Remark
529	2.921 ± 0.006	2.06 ± 0.01	23.0 ± 0.1	1950	2150	3450	0.0025	1770	a
536	2.903 ± 0.003	2.53 ± 0.02	29.8 ± 0.2	2520	2920	3530	0.0040	1870	a
526	2.896 ± 0.003	2.44 ± 0.01	27.2 ± 0.1	2270	2620	2680	0.087	2050	b
537	2.939 ± 0.003	2.63 ± 0.02	31.3 ± 0.2	2670	3090	3290 ^c	0.034	2190 ^c	c

^a Shock state.

^b Gap radiation effect.

^c Post shock state.

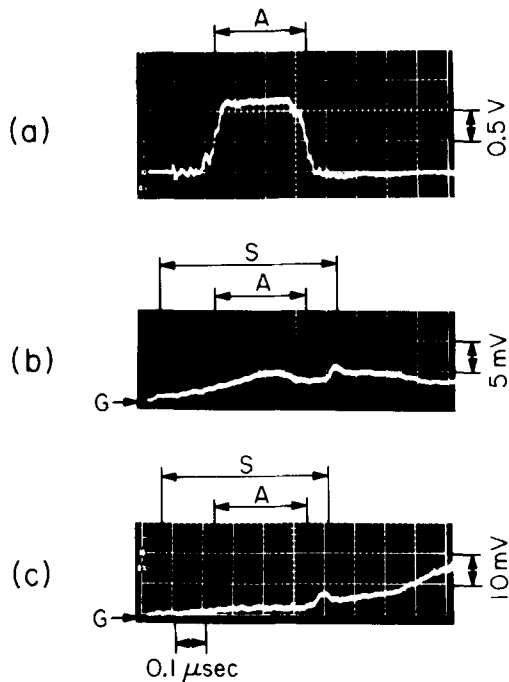


FIG. 2. Oscilloscope traces for grating pulse (a) and *PIN* photodiode output (b) and (c). (b) and (c) are at 23.0 and 29.8 GPa for shot Nos. 529 and 536, respectively. The actual voltage scale for gating pulse is 500 V/div. A, S, and G denote accumulating time, shock propagating time, and ground level, respectively. Since (b) is taken at approximately ten times higher gain of amplifier, the true intensity is lower than (c).

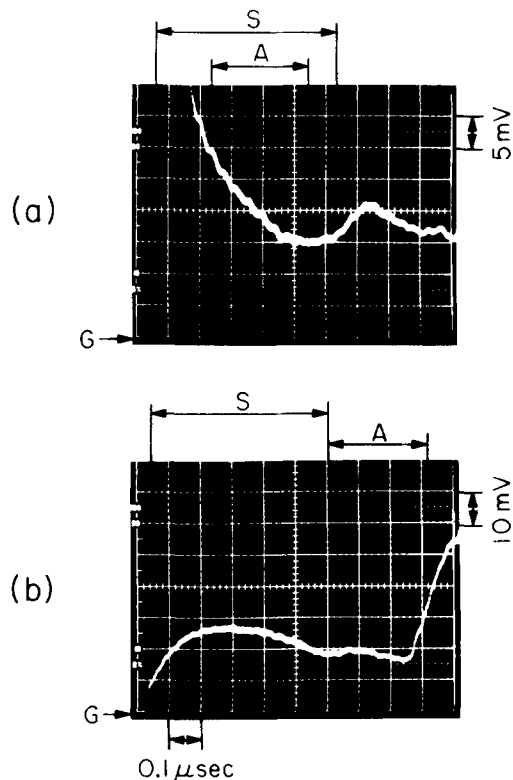


FIG. 3. Oscilloscope traces for *PIN* photodiode output at shock pressure of 27.2 and 31.3 GPa for shot Nos. 526 and 537, respectively. A, S, and G denote accumulating time, shock propagating time, and ground level, respectively. (a) was recorded for no surface preparation [case (1)].

in phase is taking place, because of the reconstructive nature and the slow reaction rate to stishovite. Moreover, the disruptive effects of shock front may accompany electroluminescence like a mechanically damaged semiconductor, which may give rise to superimpose line spectra onto a continuous blackbody spectrum.

For the thermodynamically equilibrium radiation in partially transparent material,⁹ emissivity (ϵ) depends on absorption coefficient (α), shock velocity (U_s), and propagating time (t) as follows:

$$\epsilon = 1 - \exp(-\alpha U_s t),$$

where the reflectivities are assumed to be zero. The output signals of *PIN* photodiode which we also used to monitor the present signal are too low to provide a useful comparison with the theoretical emissivity function as shown in Fig. 2. The photodiode signals do not appear to reach a level which would correspond to the emissivity of near unity.

The observation of time dependence of radiance is important not only to identify radiation mechanism but also to judge characteristics of the interface between a sample and a Cu-driver plate. For example, Fig. 3(a) (shot No. 526) shows radiance change with time for case (a) (lapped surface with presumably residual gases). It is clearly seen that extremely strong radiation occurs at shock entrance into the sample. Although both surfaces of sample and Cu-driver plates are well polished, the remaining surface topography forms an effective air gap and/or porous layer. Such gap or layer must be heated to extremely high temperature by shock compression. Evidences for this gap effect are reported elsewhere.¹³⁻¹⁵ The observed spectrum for shot No. 526 (Fig. 4) shows high spectral radiance and a good fit to Plank's equation. However, as shown in Fig. 3(a), the accumulating time of the spectral radiance overlaps with the occurrence of gap effects so that the spectral radiance is considerably high. In case (2), where an epoxy fills any gaps due to the surface roughness, the initial radiation peak is much reduced. How-

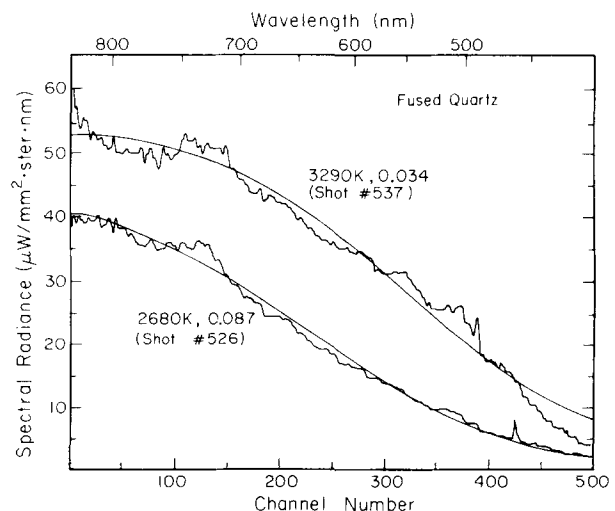


FIG. 4. Spectral radiances for shot Nos. 526 and 537 recorded with no surface preparation [case (1)] and the post shock state, respectively. The theoretical greybody curves are obtained by least squares fit. The color temperature and emissivity are indicated.

ever, the observed spectral radiance in case (2) is still considerably higher than that shown, for example, in Fig. 1. The silver coating [case (3)] appears to shield the gap radiation so this was employed here and other experiments.⁴

Both Fig. 2(b) and 2(c) show that, when the shock wave arrives at the free surface of the sample, the radiation intensity suddenly increases and yields a small peak, and that the radiance of the post shock state is greater than that of the shock state. Possible explanations of these signals are (1) that an endothermic reaction of fused quartz to stishovite could give rise to a lower shock temperature than the post shock temperature, (2) although the shock temperature is higher than the post shock temperature, the emissivity at the post shock state may be much greater than that in the shock state because the disruptive effect of free-surface motion may transform the transparent sample to translucent one, and (3) triboluminescence or electroluminescence occurs due to free-surface motion.

One measurement designed to observe the post shock state by setting a longer delay time (570 ns) was carried out (shot No. 537). However, the time-dependent profile with a large intensity was observed [Fig. 3(b)]. Such a profile has not been observed even in the other fused quartz experiments. The observed spectrum for this shot (Fig. 4) corresponds to high color temperature with low emissivity and indicates influences of some line spectra whose wavelengths correspond to those in Fig. 1. This spectrum at the post shock state is probably influenced by the unusual radiation above.

To interpret this unusual radiation, the following experiment may be suggestive. Brooks¹⁶ has observed shock-induced luminescences in fused quartz at shock pressures of 12 and 26.5 GPa, which is characterized by "window frames" of light moving in from the edges at nearly the expected cracking velocity of 2 mm/ μ s. The figure at a shock pressure of 26.5 GPa, which is in the literature,¹⁶ shows a strongly emitting area in the central portion of the sample which was interpreted as perturbations of the shock wave produced by epoxy bond.¹⁶ However, since it appears slightly later than the shock arrival at the interface, the bright spot may be intrinsic to fused quartz. In this experiment (shot No. 537), since the spot radiation occurs in the viewing slit area,

the unusual time-dependent profile would appear as in Fig. 3(b). It has been generally concluded that the heterogeneous radiation for the high color temperature with low emissivity is produced by localized deformation in brittle materials,⁴ but it is not clear how large the heterogeneity is.^{17,18} However, a kind of macroscopic heterogeneous phenomenon, which is different from a shear instability model,⁴ do occur in fused quartz, though fused quartz is of essentially uniform material. This phenomenon may be the so-called triboluminescence by which line spectra are superimposed onto the continuous blackbody spectrum. It appears to be the nature of the radiation detected.

ACKNOWLEDGMENTS

The authors appreciate the help of W. Ginn, E. Gelle, M. Long, and C. Manning of Cakteck. The work was supported by U. S. National Science Foundation, EAR78-12742.

- ¹ S. B. Korner, M. V. Sinitsyn, G. A. Kirilov, and V. D. Urlin, *Sov. Phys. JETP* **21**, 689 (1965).
- ² G. A. Lyzenga and T. J. Ahrens, *Rev. Sci. Instrum.* **50**, 1421 (1979).
- ³ H. Sugiura, K. Kondo, and A. Sawaoka, *Rev. Sci. Instrum.* **51**, 750 (1980).
- ⁴ K. Kondo and T. J. Ahrens, *Phys. Chem. Minerals* **9**, 173 (1983).
- ⁵ G. A. Lyzenga and T. J. Ahrens, *Geophys. Res. Lett.* **2**, 141 (1980).
- ⁶ G. A. Lyzenga, T. J. Ahrens, and A. C. Mitchell, *J. Geophys. Res.* (to be published).
- ⁷ H. Sugiura, Ph.D. thesis, Tokyo Institute of Technology, 1981.
- ⁸ R. G. McQueen, J. N. Fritz, and J. W. Hopson (unpublished).
- ⁹ H. Sugiura, K. Kondo, and A. Sawaoka, *J. Appl. Phys.* **53**, 4512 (1982).
- ¹⁰ H. Sugiura, K. Kondo, and A. Sawaoka, *J. Appl. Phys.* **52**, 3375 (1981).
- ¹¹ R. G. McQueen, S. P. Marsh, J. W. Taylor, J. N. Fritz, and W. J. Carter, *High-Velocity Impact Phenomena*, edited by R. Kinslow (Academic, New York, 1970), p. 244.
- ¹² K. Kondo, A. Sawaoka, and T. J. Ahrens, *J. Appl. Phys.* **52**, 5084 (1981).
- ¹³ P. A. Urtiew and R. Grover, *J. Appl. Phys.* **45**, 140 (1974).
- ¹⁴ R. Grover and P. A. Urtiew, *J. Appl. Phys.* **45**, 146 (1974).
- ¹⁵ K. Kondo and A. Sawaoka, *J. Appl. Phys.* **52**, 1590 (1981).
- ¹⁶ W. P. Brooks, *J. Appl. Phys.* **36**, 2788 (1965).
- ¹⁷ D. E. Grady, *J. Geophys. Res.* **85**, 913 (1980).
- ¹⁸ K. Kondo, A. Sawaoka, and S. Saito, *High-Pressure Science and Technology*, edited by K. D. Timmerhaus and M. S. Barber (Plenum, New York, 1979), Vol. 2, p. 905.